APPLIED PHYSICS REVIEWS—FOCUSED REVIEW

Addendum to "Fundamental questions relating to ion conduction in disordered solids"

J. Ross Macdonald[a)]

Department of Physics and Astronomy, University of North Carolina, Chapel Hill, North Carolina 27599-3255, USA

The extensive review cited in the title discusses "a number of basic scientific questions relating to ion conduction in homogeneously disordered solids" [J. C. Dyre *et al.*, Rep. Prog. Phys. **72**, 046501 (2009)]. Although it suggests answers to some of the questions raised, its main purpose is "to draw attention to the fact that this field of research still presents several fundamental challenges." This work succeeds admirably in that goal, but it does not contain reference to and discussion of some relevant published work related to the fundamental questions it discusses. It is therefore the purpose of this work to add additional information about some of these subjects, including new insights about the Barton, Nakajima, and Namikawa relation. Although most of this information is based on published papers, its omission from the cited review is an indication that it is not widely known and is therefore worth discussing. © *2010 American Institute of Physics*. [doi:10.1063/1.3359703]

TABLE OF CONTENTS

I. INTRODUCTION

In discussing the topics herein, it is useful to begin with a distinction between "relaxation" and "dispersion."[1] Although relaxation is a general term that may include dispersive effects, here I shall restrict it to processes involving only a single time constant, Debye response, and will use dispersion for ones involving more than one discrete time constant or, more usually, a continuous distribution of them, a distribution of relaxation times (DRTs). The experimental frequency response of nearly all ion-conducting solids includes one or more power-law regions with an exponent different from unity, regions exhibiting dispersion and associated with one or more DRTs. It has been found convenient and physically plausible to distinguish between a dispersion of dielectric relaxation times and one of resistive relaxation times,[1–3] although such distinction can be difficult or impossible to

infer from experimental frequency response data alone.[1,4] Here, as in Ref. 5, we primarily consider just resistive-conductive dispersion processes, ones that involve mobile charges.

II. UNIVERSAL DYNAMIC RESPONSE

The treatment of universal dynamic response (UDR) in Ref. 5 begins with a discussion of Jonscher's "universal dielectric response," power-law behavior defined by Jonscher[6] in 1977 to describe dielectric dispersion effects, and only later extended to include resistive-system dispersion and termed "universal dynamic response."[3] It may be written as

$$\sigma'(\nu) = \sigma_0[1 + (\nu/\nu_0)^n] \equiv \sigma_0[1 + (\omega\tau_0)^n], \qquad (1)$$

where in Ref. 5, $0 < n \le 1$; σ_0 is taken as σ_{dc}; and it follows that when $\nu = \nu_0$, $\sigma'(\nu_0) = 2\sigma_0$. Both the history of UDR and its utility as a fitting model are discussed in detail in Ref. 3, where it is found that not only is it a poor fitting model for bulk dispersive processes but some of the physical interpretations of its parameters are unjustified.

The original Jonscher UDR expression[6] was rewritten in the form of Eq. (1) by Almond and co-workers in 1983[7,8] but suffers from its restriction to real-part response, as opposed to a full complex expression, a failing recently discussed in general in Ref. 4. More specifically, it precludes fitting at other immittance levels such as resistivity (ρ) or electric modulus (M).

Although it seems implied in Ref. 5 that Almond and West[8] were the first to take "advantage of the frequency dependence of the conductivity," a superior, but flawed, complex version of Eq. (1),

a)Electronic mail: macd@email.unc.edu. Tel.: 919-967-5005.

     107, 101101-1

$$\sigma(\omega) = \sigma_0[1 + (i\omega\tau_{0Z})^\alpha], \qquad (2)$$

was used by Ravaine and Souquet[9] in 1973 for fitting data involving ionic conduction. Further, when Eq. (2) is transformed to the impedance (Z) or resistivity level, it is of exactly the Cole–Cole form, proposed by them in 1941 at the dielectric level for the analysis of dielectric dispersive response.[10] Thus, Eq. (2) has been termed the ZC model with $0 < \alpha \le 1$ but $\tau_{0Z} \ne \tau_0$.[3]

Both Eqs. (1) and (2) have been used for fitting conductive-system data but other models (see Sec. IV A) are nearly always superior to these, lending no support to their "universal" character or usefulness.[3] Further, they are physically incorrect in the low frequency limit where $\sigma'(\omega) - \sigma_0$ is not proportional to ω^2 in the small ω limit, as it should be and is for other dispersive fitting models discussed herein when their power-law exponents are not exactly unity, the Debye relaxation limit.

Since some $\sigma'(\nu)$ responses for LiPO$_3$ are shown and discussed in the UDR-related section of Ref. 5, it is of interest to fit a 295 K data set for this material, one kindly provided earlier by Dr. Sidebottom. To do so here, we carry out real-part and complex fits of it using the ZC model of Eq. (2) and the CZC one. Such fitting employed the LEVM complex-nonlinear-least-squares fitting program (CNLS).[11] The CZC model is appropriate for complex fits and involves a specific capacitance, the "C" in the model name, in parallel with the ZC. This capacitance plays no role in real-part ZC fits since it represents the high-frequency-limiting bulk capacitance of the material, largely associated with nondispersive dipolar effects. It may, however, include as well an effective capacitance arising from ionic motion, as discussed in Sec. IV A.

Fitting results will be summarized by values of the following fit quantities: X, S$_F$, τ_{0Z}, and α, where X is the model designation and S$_F$ is the relative standard deviation of the fit residuals. Complex fits led to ZC, 0.19, 5.3×10^{-4} s, and 0.97; CZC, 0.12, 3.1×10^{-4} s, and 0.76 (see Ref. 12 for further ZC model fitting); and the real-part fit yielded ZC, 0.15, 2.7×10^{-4} s, and 0.79. Since the Sidebottom data set was noisy, especially at low frequencies, it was fitted with the CUNS model (see Sec. IV A) and the resulting parameter estimates used to generate synthetic data well representing the original over its range. Fitting this data set led to results in agreement with those above within two or more significant figures, and the resulting complex fits are shown in Fig. 1. Note that an Eq. (1) UDR real-part fit would lead to the same results as those above for the real-part ZC fit except that its estimated τ_0 value would be appreciably less than 2.7 $\times 10^{-4}$ s [Ref. 3, see Eq. 7].

As the figure shows, the ZC fit is worst at midfrequencies and better at high ones. The high-frequency limiting log-log slopes (termed just slopes hereafter) of the CZC and ZC lines are those of their α estimates, but the actual slope of the exact data curve exceeds unity for $\log(\nu/\nu_n)$ greater than 5.75, thus not usual nearly-constant-loss (NCL) behavior. See also the discussions in Secs. III and IV D. Complex plane plots at the modulus level, as in Fig. 1(b), are often included in conductive-system data analyses and, as here,
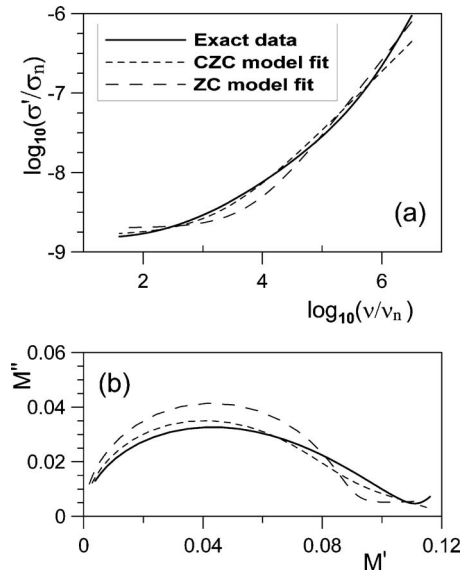

FIG. 1. (a) Log-log UDR-model fits of exact data obtained from a complex-nonlinear-least-squares CUNS-model fit of 295 K LiPO$_3$ data. The CUNS model is described in Sec. IV A. (b) Modulus-level complex plane plots of the above results. Here and elsewhere $\sigma_n = 1$ S/cm, and $\nu_n = 1$ s.

show the large departure from semicircular Debye response, and, as well, avoid the intrinsic compression of log-log presentations. Both the results of Figs. 1(a) and 1(b) make it clear that UDR-model fits are both poor and nonuniversal for the present data, also the case for other data sets.[3]

III. POLARIZATION

A. Electrode polarization effects

Electrode polarization is concerned with the blocking or partially blocking low-frequency behavior of charge carriers near an electrode. Reference 5 provides, in its Fig. 3, frequency response data sets for a lithium phosphate glass and for a Na–Ca-phosphosilicate glass at high temperature in order to illustrate electrode polarization effects. More comprehensive relevant data and fitting results were presented much earlier for $0.88 \text{ZrO}_2 \cdot 0.12 \text{Y}_2\text{O}_3$ single-crystal material at 302 and at 624 K and showed in detail both polarization effects and higher-frequency ones.[13] Of particular interest was the appearance of a log-log $\sigma'(\nu)$ maximum slope of about 1.7 for the 302 K data, much larger than that of NCL, where the slope is near unity.

Of course one would expect polarization effects to appear in series with bulk ones rather than in parallel, and a great deal of data have been fitted by a series constant-phase-element (SCPE) model expressed as $\sigma_{SC} \equiv \varepsilon_V A_{SC}(i\omega)^{\gamma_{SC}}$, where $0 \le \gamma_{SC} \le 2$ and ε_V is the permittivity of vacuum. For $\gamma_{SC} \ne 1$, it can represent the effects of rough electrodes and can, in addition, lead to high-frequency effects with a slope near $2 - \gamma_{SC}$ followed by one of γ_{SC}.[13,14] The CUNS fitting model mentioned in Sec. II and discussed in detail in Sec. IV A involves the semiuniversal bulk dispersive model, UN, in parallel with a specific capacitance C, representing the bulk, mainly dipolar, dielectric constant $\varepsilon_{D\infty}$, with both in series with $\rho_{SC} \equiv 1/\sigma_{SC}$.
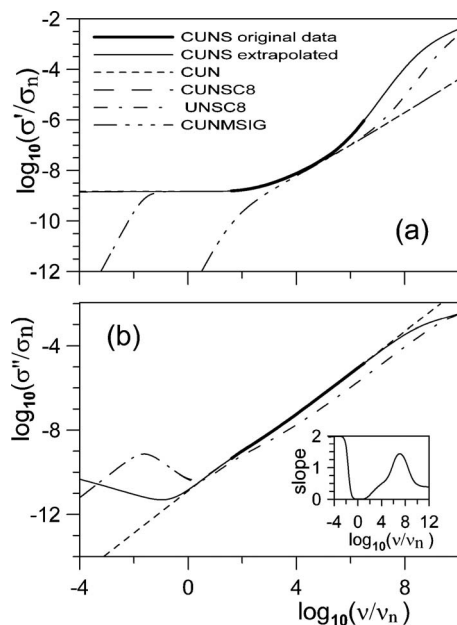
FIG. 2. Log-log plots of $\sigma(\nu)$ for the synthetic data of Fig. 1 (heavy lines) and extrapolated data using CUNS fit parameters (lighter solid lines). Other model responses shown are the two involving an additional series specific blocking capacitance of 10^{-8} F/cm, denoted by C8 in the model names (the CUNSC8 and UNSC8 ones); and for (a) only, the CUNSMSIG plot of $\sigma'_S(\nu) \equiv \sigma'(\nu) - \sigma_0$. The inset in part b shows the calculated slope of the log-log $\sigma'(\nu)$ CUNSC8 response. The UN model is the K1 one with a shape parameter value of $\beta_1 = 1/3$; the CUN one adds the bulk capacitance, represented by the $\varepsilon_{D\infty}$ dielectric constant, in parallel; and the CUNS one adds a constant phase element in series.

Since some LiPO$_3$ data plots are presented in Ref. 5, it is useful to use the parameter estimates obtained from the CUNS-model fit of the 295 K LiPO$_3$ data of Sec. II to generate wide range synthetic $\sigma(\nu)$ CUNS data. Such results are presented in Fig. 2. Here the heavy lines show the range of the original data and all others are extrapolated to both lower and higher frequencies. As discussed below, the low-frequency and high-frequency extrapolated results are consistent with experimental ones for materials with sufficiently wide frequency ranges. Note that for Fig. 2(a) the CUNS and CUN model results are the same at low frequencies, and the CUN and CUNMSIG ones are the same at high ones. In addition, CUNS and CUNSC8 are the same at high frequencies, and CUNSC8 and UNSC8 are the same at low frequencies.

The original 295 K LiPO$_3$ data do not extend to sufficiently low frequencies to allow fit estimation of a series blocking capacitor. Therefore, in order to demonstrate the effect of such a capacitor, the CUNSC8 model includes one whose size was selected to produce its effects beginning at a frequency appreciably below the lowest frequency of the Ref. 5 397 K LiPO$_3$ data, where $\sigma'(\nu)$ still remains at its σ_0 value.

The limiting low frequency slopes of both the Fig. 2(a) CUNSC8 and CUNSMSIG $\sigma'(\nu)$ responses are both 2, a value appearing in experimental data involving blocking electrodes when the measurement window extends to sufficiently low frequencies, often not the case. Although experimental data for situations with fully blocking electrodes nec-

essarily exhibit a low-frequency-limiting slope of 2, only lesser slopes, usually associated with SCPE behavior, appear when the lowest available frequency is limited. Examples of slope values of 2 or less appear in Ref. 12 (Fig. 6), Ref. 13 (Figs. 2, 3, and 5), Ref. 15 (Fig. 7), and Ref. 16 (Fig. 1).

The inset of Fig. 2(b) shows the calculated slope of the CUNSC8 model $\sigma'(\nu)$ data over a wide range. It shows a maximum slope at $\nu \simeq 1.2 \times 10^7$ Hz of about 1.44, in reasonable agreement with the $2 - \gamma_{SC}$ value of 1.62 following from the $\gamma_{SC} \simeq 0.383$ fit estimate. Although it is stated in Ref. 5 that at high frequencies a NCL regime appears for LiPO$_3$ where the slope will be close to unity and such response is identified in Fig. 3 of that work, the results shown in the inset of the present Fig. 2(b) suggest that there is no finite-range NCL region with a constant slope of near and slightly less than unity. This conclusion would have followed directly if the authors of Ref. 5 had fitted their data as in the present work and would also have been clear had the data extended to higher frequencies.

Had the measured or extrapolated frequency range extended several decades higher than shown in Fig. 2(a), the slope of the $\sigma'(\nu)$ response would have decreased to zero, a limiting plateau of $\sigma'(\nu)$ discussed in Refs. 4 and 17 but not usually apparent in most experimental data for frequencies less than a terahertz. Especially relevant is the more than 13 decade CKN data and analysis of Ref. 4 for $T = 342$ and 361 K (further discussed in Sec. IV D). Its data almost extend to such a plateau, and only a short extrapolation of the composite fit model estimated parameters leads to one.

In Fig. 2(b) the CUNSC8 and CUNS $\sigma''(\nu)$ responses are the same at high frequencies while CUNSC8 and UNSC8 ones lead to the same results at low frequencies. The frequency does not extend to sufficiently low values here to show that the CUNS line of Fig. 2(a) begins to decrease at about 10^{-5} Hz and reaches a limiting slope of just γ_{SC}. The slope of the Fig. 2(b) CUNS $\sigma''(\nu)$ line increases to a maximum at about 10^7 Hz and then also approaches the limiting slope of γ_{SC}.

Although the Fig. 2 extrapolated $\sigma'(\nu)$ and $\sigma''(\nu)$ low-end results appear at frequencies well below the measured frequency range, at higher temperatures, they will appear at higher frequencies. Both of these very low frequency responses are in accordance with those shown in Refs. 4, 12, and 13 for other materials, ones like the present that may show low frequency effects associated with a series blocking capacitor[5] and/or with SCPE behavior.[4,12,16] Even when the available $\sigma'(\nu)$ data show only a constant low frequency σ_0 region, as here and in Ref. 5, or when no such region is present,[16] CNLS fitting can nevertheless lead to a well-determined estimate of σ_0 and of the SCPE model parameters, and sometimes even to a blocking capacitor value as well.[4] We see from this discussion the power of CNLS fitting with an appropriate model as compared to the usual case of just plotting $\sigma'(\nu)$ or even $\sigma(\nu)$ data.

B. Microscopic transport models

In Ref. 5 the authors include under their section dealing with electrode polarization a discussion of microscopic trans-

TABLE I. Results of CNLS fitting of 295 K LiPO$_3$ $\sigma(\nu)$ data with several composite models. The left-most C symbol of a model name indicates the presence of a parallel $\varepsilon_{D\infty}$ bulk dielectric constant fitting parameter for the CK1 model and an ε_∞ one for the other ones. When $\varepsilon_{C1\infty}$ is nonzero, $\varepsilon_\infty = \varepsilon_{C1\infty} + \varepsilon_{D\infty}$. The S symbol at the right of the main model name designates a series constant phase element, a SCPE. The letter F indicates that a parameter is fixed, not free to vary, and p is the value of the BNN parameter for each model. The BNN p values are calculated as described in Sec. IV B, and refer to the bulk dispersion models only.

Model	100S$_F$	PDRMS	$10^{-8}\rho_0$ (Ω cm)	$10^4\tau_0$ (s)	γ_{DC} or β_k	$\varepsilon_{C1\infty}$	$\varepsilon_{D\infty}$ or ε_∞	$\Delta\varepsilon$	A$_{SC}$	γ_{SC}	p
CDC0S	6.58	0.120	5.73	9.13	0.405	$\cdots$	9.78	7.29	3.27×10^3	0.765	0.725
CK0S	5.48	0.453	6.43	3.78	0.575	$\cdots$	8.82	10.58	7.64×10^6	0.351	1.07
CK1S	5.20	0.326	6.74	0.152	0.329	1.60	7.11	15.22	4.98×10^6	0.378	1.70
CUNS	5.18	0.352	6.73	0.166	1/3 F	1.67	7.05	15.03	4.56×10^6	0.383	1.65

port models, ones that solve the Nernst–Planck small-signal ac response equations for ionic motion across a complete cell, thus more general than analysis of just electrode effects alone, except for cells of microscopic dimensions. Although they included reference to the first such analysis that required satisfaction of the Poisson equation everywhere in the cell,[18] a Poisson–Nernst–Planck (PNP) treatment, they did not mention its extension to include positive and negative charges with arbitrary valence numbers, arbitrary mobilities, and generation-recombination effects.[19] They discussed an extreme simplification of the results that ignored generation-recombination effects and the frequency dependence of the bulk conductivity, leading to an equivalent circuit that included no dispersive effects.

In contrast, the unsimplified equivalent circuit of the full situation of Ref. 19 discussed there includes such effects and is much more complicated. Although this treatment involves general boundary conditions that include the possibility of reaction and/or adsorption at electrodes, as well as the range from no blocking to full blocking,[20] for aqueous electrolytes it does not take compact and diffuse double layer effects into full account, and as mentioned in Ref. 21, it is a mean-field analysis. Detailed analyses of physical processes in the double layer began with that of Ref. 22, later extended and generalized in Ref. 23, and include a lattice gas treatment involving finite-length dipoles.[24] An important historical survey of the present field appears in Ref. 21 and includes new linear and nonlinear theoretical analyses but did not mention earlier nonlinear numerical transient response results[25] and those for a biased ac situation.[26] Although much progress in the present field has been made over the years, PNP theory still does not usually lead to small-signal ac response close to experimental results for ionic conductors, ones whose bulk response may be represented by a DRT of the kind needed to lead to good fitting of the data.

IV. FITTING MODELS

A. Composite models and the role of dimensionality

Although Ref. 5 contains no results of fitting data to a model, it does discuss the various topics of this section, particularly in reference to LiPO$_3$ data. Therefore, it is appropriate to consider CNLS fitting of such data before discussing related topics. The deficiencies of the UDR CZC model have already been illustrated in Sec. II and need no further discussion. Here, four composite bulk models that have been

found valuable for fitting of ionic conductor data are summarized and their utilities compared. They are the Davidson–Cole (DC0) model,[27] one that may be related to fractal behavior,[28] and three Kohlrausch ones, the CK0, CK1, and CUN ones, all three derived directly or indirectly from a stretched-exponential temporal dispersion correlation model.[17,29,30]

The DC0 model may be written for resistive dispersion as

$$\rho(\omega) = \rho_0/(1 + i\omega\tau_0)^{\gamma_{DC}}, \qquad (3)$$

where $0 \le \gamma_{DC} \le 1$, and, as usual, it is assumed, as also in Eqs. (1) and (2), that $\rho(\infty) \equiv \rho_\infty$ is zero or negligible. The Kohlrausch models, not generally available in closed form, are included in numerical form in the LEVM fitting program[11] and thus make possible high accuracy fitting and simulation. The K0 model involves a shape parameter β_0 whose value is equal to the high-frequency limiting slope of $\sigma'(\nu)$, while that of the K1, β_1, leads to such a slope of $1 - \beta_1$. The semiuniversal UN model is defined as the K1 with its β_1 fixed at a value of 1/3.[29]

The CK1 and CUN models include, through C, the endemic bulk high-frequency-limiting mainly dipolar dielectric constant, $\varepsilon_{D\infty}$, in parallel with the main dispersion model. These models also involve an effective dielectric constant, $\varepsilon_{C1\infty}$, arising entirely from ionic motion. For other models such as the CDC0 and CK0 ones, the C in their names denotes the full high-frequency-limiting dielectric constant, ε_∞. The parallel C is required for CNLS fitting but not, of course, for fitting of $\sigma'(\nu)$ data alone. Finally, we usually need to include a series CPE model (represented by S in the composite CUNS model) to account for electrode effects and especially for any high-frequency behavior where the $\sigma'(\nu)$ slope appreciably exceeds unity, as discussed in Secs. III A and IV D. Note that those dispersive models such as random-barrier hopping ones[5,31] and the MIGRATION model of Funke et al.,[32] which gradually approach a high-frequency-limiting $\sigma'(\nu)$ slope of unity, also require an addition to their models to represent greater slopes. Neither is readily available for fitting, and the random-barrier one has been shown to be inappropriate for data of the present type where $\beta_1 > 0.2$.[4]

Table I shows the results of fitting the original LiPO$_3$ data with the four composite models. Because the data include both appreciable random and some systematic errors, these fits lead to relatively large values of S$_F$, reducing the

ability to discriminate between them. Further, as reflected in the rms values of the relative standard deviations of the free parameters, PDRMS, the relative standard error of the A_{SC} estimates are large, especially for the bottom three models, a consequence of both errors in the data and its limited high-frequency extent. Nevertheless, it is clear that the CUNS model, with five free parameters, fits appreciably better than does the CK1S one involving six.

Especially interesting is the large difference between the estimated SCPE γ_{SC} value for the CDC0S fit and those of the other models. As mentioned in Sec. III A, SCPE response, besides often being important at low frequencies, leads to slope values of $2 - \gamma_{SC}$ at higher frequencies and a final limiting high-frequency one of γ_{SC}. Which ones appear in the available frequency window depends on the model, the extent of the data, and the value of A_{SC}. We see here that it is the small estimated value of this quantity for the CDC0S model that leads to the γ_{SC} estimate of 0.765, while the much larger A_{SC} values for the other fits are associated with a CUNS estimate of $2 - \gamma_{SC} \cong 1.62$. Had the present data extended to higher frequencies, the appropriateness of these two results would be clearer, but it is the exact CUNS data values calculated from the CUNS parameter estimates of Table I that is used for the extrapolations presented in Fig. 2.

In Ref. 5 the authors discuss some plausible choices for the ion-transport mechanism and suggest that it is a many-particle effect involving cooperation between hopping events. Feynman said "experiment is the sole judge of scientific truth," so what light do experimental results and data fitting shed on this matter? A great deal of temporal and frequency-domain data exhibits stretched-exponential response (SER), and the K0 and K1 analysis models mentioned above are derived from SER with a model shape exponent of β_k, where $k = 0$ or 1. Of these two models, the K1 is the most plausible, partly because it is uniquely derived from both macroscopic[33] and microscopic[17,34] considerations.

The original microscopic Scher–Lax model incorporated a continuous-time random walk on a regular lattice and involved hopping between randomly distributed lattice-site traps.[34] It was later specialized to involve SER,[17] thus making it isomorphic with the original K1 model.[33] In the CK1 form it has been found to fit data better than other models for a large variety of ionic-conducting materials, from glasses to such supercooled liquids as CKN.[4] To do so, it requires the addition of a parallel bulk capacitance associated with dipolar dielectric effects, and so it is designated the CK1,[29,35] a generalization not included in the incorrect but widely used original modulus formalism model, one that involves K1 alone.[33,35]

Although Ref. 5 includes an interesting discussion of the role of dimensionality in ionic conduction and states that effective dimensionality appears to be an important parameter, some relevant work on the subject is not mentioned. In particular, it has been shown that constraint theory leads a value of the β_1 shape parameter of the K1 model of 1/3, resulting in the UN model.[5,29,36] This result is consistent with the expression $\beta_k = d^*/(2 + d^*)$ for $k = 1$ when the effective dimensionality, d^*, is taken as 1, an apparent consequence of

the experimental one-dimensional electric driving field. If we define n_k as the high-frequency-limiting $\sigma'(\omega)$ power-law slope of a model or data, then $n_0 = \beta_0$ and, since $n_1 = 1 - \beta_1$, $n_1 = 2/(2 + d^*)$.

The above general formula for a SER exponent was derived in 1982 for diffusion of particles (not necessarily ions) in a d^*-dimensional isotropic space containing randomly distributed traps[37] and is thus consistent with the 1973 Scher–Lax model,[34] an approximate random-barrier approach[4] and one also involving such diffusion and trapping. For $d^* = 2$ the above formulas both predict a value of 0.5, consistent with results for some materials with two-dimensional conduction listed in Ref. 5, and also with $\beta_0 \simeq 0.5$ estimates for shell nanostructures where $d^* = 2$ is appropriate.[38,39] There is perhaps less reason to expect the $d^* = 3$ prediction of $n_0 = 3/5$ to be relevant for ionic hopping since, as discussed in Ref. 29, earlier work by Shlesinger *et al.* indicated that its value should be twice that for $d^* = 1$, leading to a value of 2/3. Limiting slopes equal to or close to 2/3 have been found for a wide variety of materials, and Ref. 5 lists some that yield values close to 1/3, 1/2, and 2/3.

B. The Barton–Nakajima–Namikawa relation

The empirical Barton–Nakajima–Namikawa (BNN) relation,

$$p = \sigma_0/(\varepsilon_V \Delta\varepsilon \omega_p), \tag{4}$$

was derived in 1966–1975, and involves a numerical constant p, the dielectric strength $\Delta\varepsilon \equiv \varepsilon_S'(0) - \varepsilon_\infty$, and a quantity $\omega_p \equiv 2\pi\nu_p$, defined below. Here, $\varepsilon_S(\omega) \equiv \sigma_S(\omega)/i\omega\varepsilon_V$, where $\sigma_S(\omega) \equiv \sigma(\omega) - \sigma_0$. The BNN relation is of interest because there is considerable evidence that when p is calculated from conductive-system experimental data it is found to be a temperature-independent quantity of order one.[40,41]

Note, however, that estimation of p requires values of σ_0, $\varepsilon_S'(0)$, ε_∞, and ω_p, and most limited-range experimental data do not lead to accurate estimates of most of these quantities and thus of p. In addition, electrode effects and response with a $\sigma'(\omega)$ high-frequency data slope near or exceeding unity can often affect a value of p calculated either from original data or from full-fit synthetic results using a composite model. Then, such a p estimate is not fully representative of that of the main dispersive process present in the data. Alternatively, if the full data are accurately fitted by a composite model involving a dispersed part A, then estimated model-A parameter values of the fit may be used to generate synthetic data that leads to accurate values of p for that model, the route followed herein. Thus, here we present accurately calculated values of p for the DC0, K0, K1, and UN models alone.

The quantity ω_p is defined in Ref. 5 as the "angular frequency marking the onset of ac conduction," one generally defined by the relation $\sigma'(\omega_O) = 2\sigma_0$, or equivalently, $\sigma_S'(\omega_O) = \sigma_0$; thus for this definition $\omega_p = \omega_o$. In most previous work, however, ω_p is taken to be the value at the peak of the $\varepsilon_S''(\omega)$ dielectric loss curve,[29,41] the present definition and that leading to all the results herein. Because $\omega_p \equiv 2\pi\nu_p$ and ω_O

TABLE II. BNN quantities for three fitting models with unity parameter values for several exponent choices. The values shown here are rounded, but frequency values were calculated to five or more significant figures.

Model	γ_{DC} or β_k	$\Delta\varepsilon$	ν_O (Hz)	ν_p (Hz)	ν_O/ν_p	p
DC0	2/3	2/3	0.981	1.027	0.955	0.233
DC0	0.5	0.5	1.103	0.655	1.683	0.486
DC0	1/3	1/3	1.862	0.481	3.875	0.993
K0	2/3	0.1329	0.541	0.186	2.901	0.643
K0	0.5	2	0.443	4.99×10^{-2}	8.875	1.60
K0	1/3	6	0.467	4.88×10^{-3}	95.73	5.44
K1	0.37	24.88	3.56×10^{-2}	4.32×10^{-3}	8.251	1.48
K1=UN	1/3	54	1.752×10^{-2}	1.79×10^{-3}	9.813	1.65
K1	0.3	130.7	7.81×10^{-3}	6.47×10^{-4}	12.06	1.88

$\equiv 2\pi\nu_O$ may not be closely the same, however, it is worthwhile to estimate them for the various fitting models considered herein.

For simplicity in calculation, we set values of σ_0, τ_0, and ε_V to unity for each model and express its frequencies in hertz. Alternatively this approach may be interpreted as a scaling that leads to these unity values. Here $\sigma_0=1$ S/cm is subtracted at the admittance level, and the frequency calculated from τ_0 is just $\nu_\tau=(2\pi)^{-1}$ Hz. It follows that for this situation $\sigma'_S(\nu_O)=1$, the definition of ν_O, and therefore $p=1/(2\pi\nu_p\Delta\varepsilon)$. Next, many model values of $\sigma'_S(\nu)$ and of $\varepsilon''_S(\nu)$ are calculated to accurately estimate ν_O and ν_p, respectively. This is particularly important for situations where $\varepsilon''_S(\nu)$ exhibits a broad peak, such as that for the UN model. For the present normalized models, $\Delta\varepsilon=\gamma_{DC}$ for the DC0 one and $\Gamma(1/\beta_0)/\beta_0$ for the K0 model. For both these models ε_∞ is identically zero, but for the K1, this is not the case and so $\Delta\varepsilon\equiv\varepsilon'_S(0)-\varepsilon_\infty=\{\Gamma(2/\beta_1)/\Gamma(1/\beta_1)\}-\Gamma(1/\beta_1)/\beta_1$, where Γ is the Euler gamma function.

Table II and Fig. 3 show BNN-related results for models with unity parameter values as discussed above. Table II makes it clear t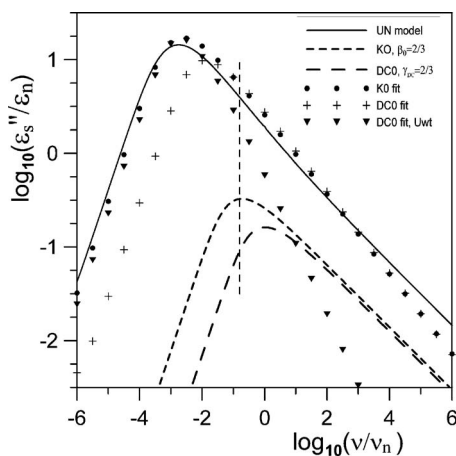hat for most situations, values of ν_p and ν_O are quite different, and ν_O is not a proper choice for calculating p for the present models. Figure 3 shows the differences in the $\varepsilon''_S(\nu)$ responses for the UN, K0, and DC0 models. With the choice of 2/3 for the DC0 and K0 exponents and 1/3 for the K1=UN model, we see that the high-frequency limiting slope for all three is just $-2/3$, consistent with the often found limiting experimental-data power-law slope of 2/3 for $\sigma'(\nu)$. It is interesting that the UN ν_p value is much less than that of ν_τ, while they are nearly equal for the K0 one, and ν_p is appreciably larger for the DC0 one. The fitting results shown by symbols alone make it clear that although the K0 model does not fit the UN data well, the DC0 one with either proportional or unity weighting leads to a far worse fit.

Figure 4 shows how p depends on the characteristic exponent values of the K0, DC0, and K1 models. It is remarkable how little the p of the K1 model varies with its β_1 exponent and remains near unity. As suggested by Gunnar Niklasson, trustworthy estimates of p calculated directly from experimental data could be quite helpful in selecting, or eliminating, an appropriate fitting model.

The results in Table II and Fig. 4 make it clear that unless the γ_{DC} and β_K shape-parameter exponents are temperature independent, not the usual situation for most of
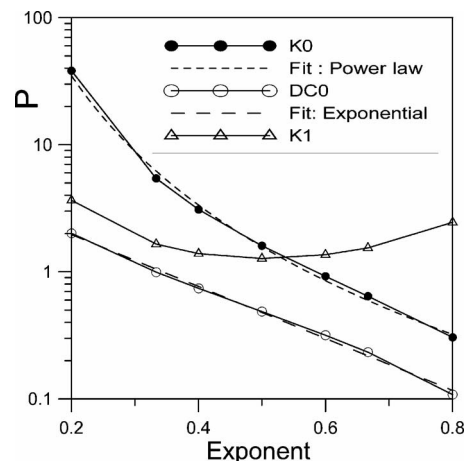

FIG. 3. Log-log plots of $\varepsilon''_S(\nu)$ for unity values of the model parameters σ_0 and τ_0, and for ε_V. The exponent values of the K0 and DC0 models are 2/3 here. The vertical dashed line indicates the resulting value of ν_τ that corresponding to $\sigma_0=1$ S/cm. The results shown only by symbols are those resulting from fitting the $\varepsilon''_S(\nu)$ part of the UN model data, the first two with the usual choice of proportional weighting and the second DC0 one with unity weighting.

FIG. 4. Plots of accurate values of the BNN p parameter vs values of the characteristic shape parameter exponents, β_0, γ_{DC}, and β_1, of the K0, DC0, and K1 models, respectively. Fits of two of these responses are also included.

them, p will not be and so will not be a constant, as required by its definition. The situation is different, however, for the $\beta_1 = 1/3$ UN model. Since it fits much data for which a single species of ion is mobile, its temperature-independent value of $p = 1.65$ is probably the most appropriate one. In hopping simulations,[41] p was found to fall in the range 1.5 ± 0.4, consistent with the UN value of 1.65.

Finally, consider the microscopic PNP model of a cell involving equal ionic mobilities, equal valence numbers, and full dissociation for a completely blocking situation [Refs. 19 and 42, Eq. (1)]. An important parameter of this model is M, the number of Debye lengths in a half-cell length, and it is found that the value of the BNN p parameter is unity for $M \geq 100$, is about 1.07 at $M = 10$, and only reaches 1.20 at $M = 1$. The epsilon-level complex plane plot of this model, for M as large or larger than 10, appears close to that of Debye response but involves a nonzero geometrical bulk capacitance, represented by $\varepsilon_{D\infty}$, in the high-frequency limit and a standard double-layer low-frequency-limiting capacitance. Since the model is blocking, its dc conductivity is zero and its high frequency limit, $\sigma'(\infty)$, is the inverse of its ρ_∞ parameter, with no region of increase beyond the $\sigma'(\infty)$ plateau. For fitting data the PNP model will therefore usually require the addition of a SCPE or other dispersive model. The PNP-response model is available in the LEVMW computer program,[11] and its behavior and possible usefulness for fitting data from a variety of different materials is further discussed in pending work of the author.

C. Time-temperature superposition

Time-temperature superposition (TTS) is usually defined as temperature-independent behavior of a log-log plot of $\sigma'(\omega)$ when individual data sets are suitably scaled. Further, in Ref. 5 it is stated that TTS applies to "all single-ion-conducting glasses and crystals with structural disorder." It should be noted, however, that TTS plots are almost invariably presented for limited-range $\sigma'(\omega)$ data which show neither low-frequency electrode effects nor high-frequency slopes exceeding unity and for which σ'_{max}/σ_0 rarely exceeds 2.5 decades (e.g., Fig. 5 of Ref. 5 for LiPO$_3$). For the present 295 K LiPO$_3$ data, however, the results in Figs. 1 and 2 confirm that the maximum high-frequency slope exceeds unity, and it is likely that electrode polarization effects, more obvious at low frequencies for $\sigma''(\omega)$ plots than for $\sigma'(\omega)$ ones, as shown in Fig. 2, are indeed present for this material, as one would certainly expect for non-parent-ion electrodes.

In the section on TTS in Ref. 5, it is stated that for experimental data $\sigma'(\omega) - \sigma_0$ becomes proportional to ω in the low-frequency limit. In fact, it is proportional to ω^2, in agreement with the results of Fig. 2. Such proportionality is indeed a feature of all reasonable fitting models, thus excluding those such as the UDR, ZC, and Havriliak–Negami ones.

Verification of TTS requires separate scaling of both $\sigma'(\omega)$ and ω.[5,29,43] Over the years several different scaling choices have been proposed and used, and Ref. 5 includes a valuable discussion of open questions about TTS. In addition, Refs. 29 and 43 discuss scaling possibilities for other immittance levels than just $\sigma'(\omega)$ and the more general and powerful alternative to scaling provided by direct CNLS fitting of data at any immittance level by specific models. The conditions under which $\sigma'(\omega)$ TTS behavior is demonstrated suggest that it is usually associated with a single dispersion process, since NCL and/or partial blocking electrode effects, when well represented by a series constant-phase element, as discussed below in Sec. IV D, are temperature dependent in ways that may not be well compensated by ordinary scaling approaches.

The above considerations suggest that one might expect TTS behavior for data well represented by a single dispersion model under appropriate conditions.[43] Such models usually involve just three free parameters: their dc conductivity, σ_0, a characteristic relaxation time, τ_0, and a shape parameter. As discussed earlier herein, the shape parameters for the DC0, K0, and K1 models are γ_{DC}, β_0, and β_1, respectively. If one of them depends appreciably on temperature, that model will not lead to TTS or to a temperature-independent value of the BNN p.

There are few if any temperature-dependent CNLS fitting results for the DC0 model, and also little available for the K0 model, one not even recognized by those who use the K1 but not the CK1 model.[33,35] However, estimated composite-model fit values of β_0 decrease with increasing temperature over the range of 464 K to 583 K for $0.88\text{ZrO}_2 \cdot 0.12\text{Y}_2\text{O}_3$, while those for β_1 remain constant and close to 1/3.[44] It therefore seems likely that of these three models the only one whose shape parameter does not depend appreciably on temperature is the specific K1 model where it is found that, for a large amount of data for materials with a single species of mobile ions, $\beta_1 \cong 1/3$, the UN one. Not only is β_1 found to be temperature independent over an appreciable range, but it is also found to be independent of ionic concentration under constant stoichiometry conditions.[29,44]

For most thermally activated materials that involve Arrhenius behavior, the activation energies of $T\sigma_0$ and τ_0 are found to be identical or very close to the same. When this is the case, if one scales $\sigma(\omega)$ with $T\sigma_0$ and uses $\omega\tau_0$ in place of ω, then for the three-parameter dispersive models listed above, the only remaining possible temperature dependence is that of the shape parameter. It thus follows that of the above appropriate models, the only one that may be expected to exhibit TTS is the UN one, one that leads to a value of the BNN p parameter close to values calculated from the data for a wide variety of materials.[41] Note that, as shown in the previous section, there are appreciable differences in the values of ν_τ, ν_O, and ν_p, so scaling with the radial frequency corresponding to either of the last two, a common practice, is less appropriate than that involving τ_0.

It is noteworthy that it has been shown that TTS and analyticity of the scaling function imply the BNN relation but not a specific value of p.[5,41] Since the UN model is the only one of those considered here that leads to TTS behavior when its results are scaled and, as well, to a plausible value of p, it seems likely that all previously published scaled $\sigma'(\omega)$ data that led to TTS might be well fitted by the UN model over an appreciable frequency range. Full complex fitting of the corresponding $\sigma(\omega)$ data sets would require,

however, a composite CUN or possibly even a CUNS model. Since accurate calculation of p requires a good fit of a known model in any case, it seems that such fitting obviates the need for calculating p. Finally, accurate CNLS fitting of an appropriate model yields estimates of all parameter values relevant to the dispersive processes present and thus yields a multidimensional description of it, far more useful and general than a one-dimensional test of the applicability of TTS.

D. NCL behavior

NCL often appears in $\varepsilon''(\nu)$ conductive-system data at high frequencies and/or low temperatures and is usually characterized by a near-zero slope of $\varepsilon''(\nu)$ and a corresponding $\sigma'(\nu)$ slope near unity over an appreciable frequency range. This range is bounded by conductive-system dispersion on the lower side until it becomes of negligible influence at low temperatures in the available frequency range, and by the eventual approach of $\sigma'(\nu)$ to a constant plateau region at very high frequencies.[4,17] In Ref. [5], NCL is identified as a regime where the slope of $\sigma'(\nu)$, there denoted by n, satisfies $n \cong 1$, and the question is asked whether n can be slightly less than 1, equal to 1, or slightly greater. The equality condition for a nonzero frequency span was shown in Refs [4], [14], and [45] to be inapplicable. Further, as we have seen, the $\sigma'(\nu)$ slope may appreciably exceed unity at high frequencies. Therefore, NCL should be defined as a frequency region of nonzero length where the $\varepsilon''(\nu)$ slope is close to zero but one without an actual value of 0.

Reference [5] includes a valuable discussion of several possible physical processes whose presence might explain NCL. Of particular interest is the suggestion of relaxation of a system over an energy barrier involving an asymmetric double-well potential. Another possibility is the vibration at high frequencies of ions fully or partly trapped in a slightly leaky potential-barrier cage, a process usually considered distinct from vibrational behavior associated with the bulk dielectric constant $\varepsilon_{D\infty}$, and the plateau resistivity possibly appearing at even higher frequencies.[4,17]

A perennial question, raised but not settled in Ref. [5], is the degree to which hopping ions may contribute to NCL. Since 1994,[45] much work has been devoted to exploring this possibility. In the 1994 paper, a parallel combination of a conductive-system dispersive model and a dielectric dispersion one was discussed, and it was also shown that using just an approximate effective-medium, random-barrier conductive-system model, the BDM, led to all the usual features of experimental $\sigma'(\nu)$ data over a 15 decade frequency window. In particular, at high temperatures dc response was followed by a dispersive region whose slope approached unity at high frequencies, and at sufficiently low temperatures it reduced to just a line of nearly unity slope over the whole frequency span.

Later, further work was devoted to comparing the appropriateness of the inclusion of a NCL constant-phase element in either parallel or series with a conductive-system dispersive model, such as the K1.[13,14,43,46,47] Particularly interesting was the result that a CUNS model could lead to a $\varepsilon''(\nu)$ slope of -0.02 to $+0.02$ over an range of six decades,[16] and an effective-medium model involving $\varepsilon_{D\infty}$ and a parallel CPE led to nearly zero $\varepsilon''(\nu)$ slope over 12 decades.[47] Of course, other processes will dominate to reduce these extreme ranges to the smaller ones that are actually observed.

The inclusion of a series CPE, as in the CK1S and CUNS models, is of especial importance because the SCPE element is usually added to a model to represent all or part of its low-frequency electrode polarization. But it was shown in Refs. [13] and [14] that such addition could lead as well to high-frequency effects, including NCL ones (see the present Sec. III A). To the degree that good fitting of experimental data for both regions is found, as well as that for the ordinary conductive-system dispersion region between them, it seems clear, but surprising, that both responses must involve the same mobile charges, modeled by the series CPE but likely involving different kinds of motion at low and high frequencies.

A particularly instructive example is that of the fitting results for very-wide-frequency-range data of supercooled liquid $0.4Ca(NO_3)_2 \cdot 0.6KNO_3$ (CKN) at 342 K and 361 K.[4] A composite model involving CK1S elements fitted the data well, including both electrode polarization and NCL regions. Further, the estimated value of γ_{DC} increased toward unity as the temperature decreased. The smaller temperature dependence of the SCPE elements as compared to those of the K1 implies that, as the temperature is lowered under constant-structure conditions, the K1 dispersion will become negligible in the available frequency window, and only the SCPE response will remain and will approach a limiting NCL $\sigma'(\nu)$ slope of unity. Mobile-charge explanations of NCL, such as those discussed here, have been little considered by others but evidently deserve further attention to further elucidate this kind of response.

ACKNOWLEDGMENTS

[1] J. R. Macdonald, J. Phys. Chem. B **112**, 13684 (2008).
[2] J. R. Macdonald, Braz. J. Phys. **29**, 332 (1999).
[3] J. R. Macdonald, Solid State Ionics **133**, 79 (2000).
[4] J. R. Macdonald, J. Phys. Chem. B **113**, 9175 (2009).
[5] J. C. Dyre, P. Maass, B. Roling, and D. L. Sidebottom, Rep. Prog. Phys. **72**, 046501 (2009).
[6] A. K. Jonscher, Nature (London) **267**, 673 (1977).
[7] D. P. Almond, G. K. Duncan, and A. R. West, Solid State Ionics **8**, 159 (1983).
[8] D. P. Almond and A. R. West, Solid State Ionics **11**, 57 (1983).
[9] D. Ravaine and J.-L. Souquet, CR Acad. Sci. (Paris) **277C**, 489 (1973); see also the comprehensive review by E. T. McAdams and J. Jossinet, Physiol. Meas. **16**, A1 (1995) of relevant earlier work in this area going back to at least 1897.
[10] K. S. Cole and R. H. Cole, J. Chem. Phys. **9**, 341 (1941).
[11] J. R. Macdonald and L. D. Potter, Jr., Solid State Ion. **24**, 61 (1987); J. R. Macdonald, J. Comput. Phys. **157**, 280 (2000) (The newest WINDOWS version, LEVMW, of the comprehensive LEVM fitting and inversion program may be downloaded at no cost by accessing http://jrossmacdonald.com. It includes an extensive manual and executable and full source code. More information about LEVM is provided at this internet address. All of the Macdonald papers cited herein are also available in PDF format for downloading from this address.).
[12] J. R. Macdonald, J. Phys.: Condens. Matter **17**, 4369 (2005).
[13] J. R. Macdonald, J. Non-Cryst. Solids **307–310**, 913 (2002).

[14] J. R. Macdonald, J. Chem. Phys. **115**, 6192 (2001).

[15] J. R. Macdonald, *Electrically Based Microstructural Characterization*, MRS Symposia Proceedings Vol. 411 (Materials Research Society, Pittsburgh, PA, 1996), pp. 71–83.

[16] J. R. Macdonald and M. M. Ahmad, J. Phys.: Condens. Matter **19**, 046215 (2007).

[17] J. R. Macdonald, Solid State Ionics **150**, 263 (2002), the symbol $\rho_{C1\infty}$ at the left side of the equation above Fig. 6 on p. 274 should be replaced by $\tau_{C1\infty}$.

[18] J. R. Macdonald, Phys. Rev. **92**, 4 (1953).

[19] J. R. Macdonald and D. R. Franceschetti, J. Chem. Phys. **68**, 1614 (1978).

[20] J. R. Macdonald, J. Electrochem. Soc. **135**, 2274 (1988).

[21] M. Z. Bazant, K. Thornton, and A. Ajdari, Phys. Rev. E **70**, 021506 (2004).

[22] J. R. Macdonald, J. Chem. Phys. **22**, 1857 (1954).

[23] J. R. Macdonald and C. A. Barlow, Jr., J. Chem. Phys. **36**, 3062 (1962).

[24] J. R. Macdonald and S. W. Kenkel, J. Chem. Phys. **80**, 2168 (1984).

[25] D. R. Franceschetti and J. R. Macdonald, J. Appl. Phys. **50**, 291 (1979).

[26] D. R. Franceschetti and J. R. Macdonald, J. Electroanal. Chem. **100**, 583 (1979).

[27] D. W. Davidson and R. H. Cole, J. Chem. Phys. **19**, 1484 (1951).

[28] R. Nigmatullin and Ya. E. Ryabov, Phys. Solid State **39**, 87 (1997).

[29] J. R. Macdonald, Phys. Rev. B **71**, 184307 (2005).

[30] J. R. Macdonald, J. Phys.: Condens. Matter **18**, 629 (2006).

[31] T. B. Schrøder and J. C. Dyre, Phys. Rev. Lett. **101**, 025901 (2008).

[32] K. Funke, P. Singh, and R. D. Banhatti, Phys. Chem. Chem. Phys. **9**, 5582 (2007).

[33] C. T. Moynihan, L. P. Boesch, and N. L. Laberge, Phys. Chem. Glasses **14**, 122 (1973).

[34] H. Scher and M. Lax, Phys. Rev. B **7**, 4491 (1973).

[35] J. R. Macdonald, J. Phys. Chem. Solids **70**, 546 (2009).

[36] J. R. Macdonald and J. C. Phillips, J. Chem. Phys. **122**, 074510 (2005).

[37] P. Grassberger and I. Procaccia, J. Chem. Phys. **77**, 6281 (1982).

[38] B. Ghosh, D. Chakravorty, J. R. Macdonald, and G. C. Das, J. Appl. Phys. **99**, 064307 (2006).

[39] S. Basu, J. R. Macdonald, and D. Chakravorty, J. Mater. Res. **21**, 1704 (2006).

[40] J. C. Dyre, J. Non-Cryst. Solids **135**, 219 (1991).

[41] J. C. Dyre and T. B. Schrøder, Rev. Mod. Phys. **72**, 873 (2000).

[42] J. R. Macdonald, J. Electroanal. Chem. **32**, 317 (1971); below Eq. A-1, in γ_j replace θ_j^2 by θ_j, and on p. 2279 in t_1 replace ψ by $\psi^{1/2}$.

[43] J. R. Macdonald, J. Appl. Phys. **90**, 153 (2001).

[44] J. R. Macdonald, J. Chem. Phys. **116**, 3401 (2002).

[45] J. R. Macdonald, Appl. Phys. A: Solids Surf. **59**, 181 (1994).

[46] J. R. Macdonald, Phys. Rev. B **66**, 064305 (2002).

[47] J. R. Macdonald, J. Appl. Phys. **94**, 558 (2003).